Influence of Freezing Layer on the Crystallization Kinetics of PCL on Oriented PE Film

Hao Zhang[a*], Ying-Xiao Song[a], Na Li[a], Shao-Juan Wang[a], Jian Hu[a], Rui Xin[a], Jie Zhang[b], Chun-Feng Song[b], and Shou-Ke Yan[a,b*]

[a] *Key Laboratory of Rubber-Plastics, Ministry of Education/Shandong Provincial Key Laboratory of Rubber-Plastics, Qingdao University of Science & Technology, Qingdao 266042, China*
[b] *State Key Laboratory of Chemical Resource Engineering, Beijing University of Chemical Technology, Beijing 100029, China*

Ⓔ Electronic Supplementary Information

Abstract The effect of freezing layer on the crystallization kinetics of poly(ε-caprolactone) (PCL) thin and ultrathin films was investigated by monitor the growth process of it on oriented polyethylene (PE) and CaF$_2$ with and without freezing layer, respectively. It was found that the PCL films with similar thicknesses crystallize much faster on oriented PE than on CaF$_2$ substrate. For example, the crystallization rate constant of a 102 nm thick PCL film decreases tremendously by 3 orders of magnitude from 1.1×10^{-1} on PE substrate at 50 °C to 7×10^{-4} on CaF$_2$ surface at 40 °C. Moreover, the crystallization of PCL accelerates on CaF$_2$ surface while slows down at PE surface with increasing film thickness. The ultrathin films of PCL with thickness less than 14 nm exhibits the fastest crystallization rate on oriented PE with a rate constant of about 3.5×10^{-1}, which is 3 times higher than that of a *ca*. 50 nm thick film. This illustrates the great influence of freezing layer on the crystallization process of PCL. The freezing layer thickness of PCL on PE is estimated to be in the range of 14−17 nm. Taking the radius of gyration ($R_g \sim 15.6$ nm) of the used PCL material into account, the obtained results may imply the existence of a correlation between the R_g of PCL and its freezing layer thickness at PE substrate.

Keywords Poly(ε-caprolactone); Polyethylene; Interface; Freezing layer; Crystallization kinetics

INTRODUCTION

The property and functionality of polymeric materials depend seriously on their chemical and multiscale condensed structures.[1–10] As more than two thirds of synthetic polymers can crystallize under suitable conditions, great efforts have been contributed to study the crystallization behavior of polymers for the sake of control their crystal structures and crystalline morphologies.[11–15] Among many others, surface-induced epitaxial crystallization has been proved to be effective in regulating both crystal structure and morphology of semicrystalline polymers.[16–26] For polymer epitaxy, most widely researched issues are the mutual crystal orientation relationship of the deposit polymer with the used underlying substrate and the related mechanism of it. Up to date, great progress on the understanding of epitaxial crystallization mechanism at a molecular level and related controlling factors has been achieved through extensive studies on the final mutual orientation relationship of different epitaxial polymer pairs *via* X-ray diffraction, atomic force microscopy, and transmission electron microscopy combined with electron diffraction.[27–30] It is widely accepted that the unique mutual orientation and specific crystal form selection are determined by the existing crystallographic matching between the epitaxial pairs in the contacting planes.[27,28]

It should be noted that the substrate-induced epitaxial organization of deposit polymer should start unambiguously at the surface of the oriented substrate. However, a visualization of the organization of deposit polymer directly at the substrate surface is impossible due to the interface is buried between the melt of deposit polymer and the solid substrate. Fortunately, the elegant technique developed by Thurn-Albrecht *et al*.[31–36] helps to disclose the existence of an ordered wetting layer at the interface of several polymers, such as polyethylene (PE),[31–33] poly(ε-caprolactone) (PCL),[33–35] and poly(ethylene oxide) (PEO),[36] onto highly ordered pyrolytic graphite or MoS$_2$ substrates successfully. The wetting layer, referred to as freezing layer, is confirmed to be stable above the bulk melting temperature and exerts

* Corresponding authors, E-mail: zhanghao@qust.edu.cn (H.Z.)
                                              E-mail: skyan@mail.buct.edu.cn (S.K.Y.)

great influence on the crystallization kinetics of the polymers. This implies that the crystallization kinetics of polymers within the freezing layer and outside the freezing region must be quite different. This has, however, not been studied, even though abundant researches have been denoted on the molecular dynamics of thin (thickness between 100–1000 nm) and ultrathin (thinner than 100 nm) polymer films at solid surfaces without special crystallographic interaction.[37−44]

In this work, the PCL has been chosen as a model system for studying the influence of the freezing layer on its crystallization kinetics. To this end, oriented PE and CaF_2 were selected as the substrates of it. It is well confirmed that ordered chain organization of PCL on PE takes place at temperatures above its nominal melting point,[45,46] reflecting the existence of a freezing layer of PCL. On the other hand, CaF_2 cannot induce epitaxial crystallization of PCL and thus oriented chain organization of PCL does not occur. The crystallization kinetics of PCL films with different thickness at oriented PE and CaF_2 surfaces was followed by Fourier transform infrared (FTIR) spectroscopy, which had widely been used to characterize the crystallization and glass transition behavior of polymers.[47−50] The results show not only the crystallization kinetic but also the film thickness dependence of PCL at PE surface is quite different from that at CaF_2 substrate. For example, with increasing film thickness, the crystallization rate of PCL increases on CaF_2 substrate but decreases at PE surface. It seems that the freezing layer thickness of PCL on PE substrate correlates with its radius of gyration (R_g). The purpose of this paper is to display the detailed experimental results and reasonable explanations for the different film thickness dependence of PCL crystallization kinetics on PE and CaF_2 substrates. We hope this will shed more light on the different molecular organization behavior of thin and ultrathin polymer films at different flat solid surfaces.

EXPERIMENTAL

Materials
Commercial grade PCL, weight-average molecular weight M_w~6.9×10^4 g/mol, was purchased from Sigma-Aldrich Co. High-density polyethylene (HDPE 7000f) was produced by Ilam Petrochemical Co., Iran. Commercial ethyl acetate and xylene solvents were used as received.

Sample Preparation
Highly oriented thin PE films were prepared according to a melt-draw technique invented by Petermann and Gohil.[51] The structure of melt-drawn PE ultrathin films of *ca.* 50 nm in thickness has frequently been shown in previous publications.[52−56] It will therefore not be presented here in this paper again. The samples used for studying the dynamics of epitaxial crystallization of PCL on highly oriented PE substrate adopt a sandwich configuration for increasing their contact area so that enhancing the FTIR signal. They were prepared by first spin-coating PCL ethyl acetate solution at different concentrations onto oriented PE film supported by highly polished CaF_2 substrate and then covered by another piece of oriented PE film. The use of polished CaF_2 as supporting substrate is for a better repeatability of the experiments. The thicknesses of PCL films are measured by Bruker DektakXT

profilometer as 19±2, 28±1, 34±2, 102±5, 160±8, 1000±20 and 2000±50 nm. The samples thicker than 34 nm were directly used for FTIR study, while the samples with PCL film thinner than 34 nm were multilayer stacked to enhance the FTIR signal of PCL.

Characterization
For FTIR experiments, a Bruker VERTEX70 spectrometer was used. FTIR spectra in the wavenumber range from 400 cm^{-1} to 4000 cm^{-1} were obtained by averaging 32 scans at a 4 cm^{-1} resolution and recorded after every 60 s. For crystallization kinetic study, the PE/PCL/PE samples were first heated up to 85 °C (below the melting point of PE but above that of PCL) for 15 min and then cooled down to 50 °C for isothermal crystallization. To show the different influence of CaF_2, the crystallization kinetics of pure PCL thin films with similar thicknesses at CaF_2 surface was also performed by melting the PCL films at 85 °C for 15 min and then crystallized isothermally at 40 °C. The reason for the use of a lower crystallization temperature for PCL/CaF_2 is that the crystallization of PCL ultrathin films on CaF_2 substrate at 50 °C is hardly possible. Even at 40 °C, the crystallization of PCL ultrathin films (<100 nm) is too slow to be followed. Therefore, only the PCL thin films thicker than 100 nm have been employed to follow the crystallization kinetics of PCL on CaF_2 substrate. Nevertheless, it is well-known that the crystallization rate of PCL above 40 °C gets slower with increasing temperature. In this case, the higher the T_c, the slower the crystallization rate. Consequently, the influence of crystallization temperature on the kinetic does actually not affect the conclusion of present experimental data analysis.

RESULTS AND DISCUSSION

For reasonable infrared spectroscopic analysis, correct FTIR band assignments of PCL are necessary. It is well documented that the band at 731cm^{-1} is crystalline sensitive, while the other bands, such as 1295, 1245 and 1192 cm^{-1}, are conformational sensitive.[45] In the present work, as mentioned in the experimental part, highly polished CaF_2 substrate was used for a better repeatability. Fig. 1(a) shows the FTIR spectra of a PCL film on CaF_2 substrate before and after crystallization. It can be seen that the transmittance of CaF_2 is poor below 1100 cm^{-1}. Therefore, the data analysis of 731 cm^{-1} band is tricky and thus not suitable for analyzing the crystallization process. Phillipson *et al.*[57] reported the use of carbonyl absorption band at 1724 cm^{-1} for measuring the PCL crystallinity quantitatively with time, owing to its high intensity and isolation (see Fig. 1b). Consequently, the 1724 cm^{-1} band instead of 731 cm^{-1} band was adopted here to monitor the crystallization dynamics of PCL with varied thickness on CaF_2 and oriented PE substrates. In this way, the relative crystallinity of PCL was calculated by ($A_t − A_0$)/($A_\infty − A_0$), with A_0 represents the intensity of 1724 cm^{-1} band at the time just cooling the sample from 85 °C down to crystallization temperature, whereas A_t and A_∞ represent the band intensities after t time and end crystallization of PCL, respectively.

Fig. 2(a) shows the change of relative crystallinity as a function of time for a ~1 μm thick PCL film sandwiched between oriented PE substrates crystallized isothermally at 50 °C. From Fig. 2(a), it is obvious that the crystallization of PCL sand-
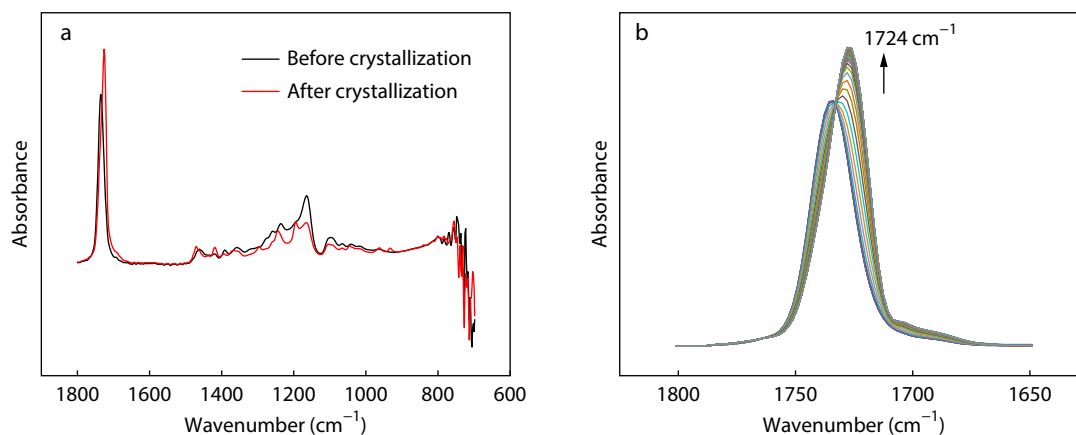
Fig. 1 (a) FTIR spectra of a thick PCL film before and after isothermal crystallization on CaF_2 substrate at 40 °C; (b) Crystallization time dependent intensity variation of 1724 cm^{-1} band. The arrow indicates the direction of band intensity change with time.
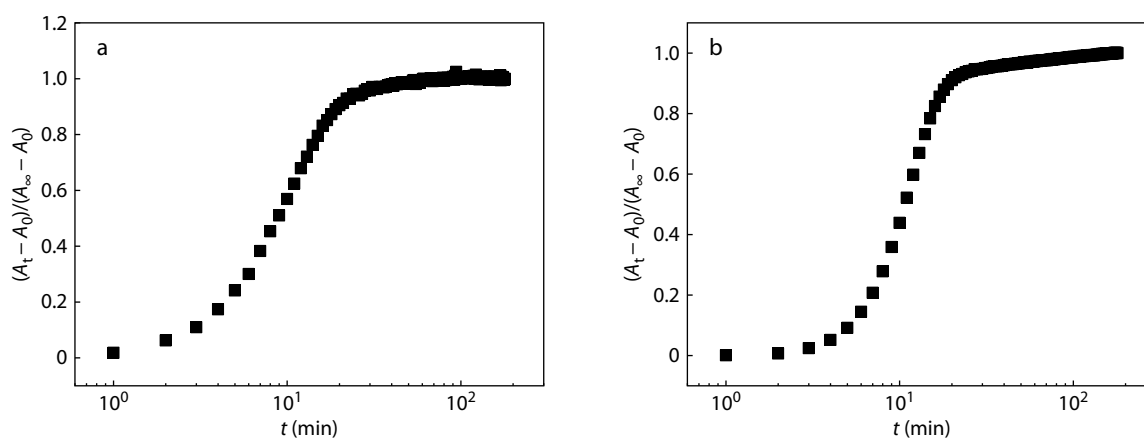

Fig. 2 Time-dependent relative crystallinity changes of a PCL thin film with 1 μm in thickness sandwiched between two oriented PE substrates during isothermal crystallization at 50 °C (a) and on CaF_2 substrate during isothermal crystallization at 40 °C (b).

wiched between PE substrates starts immediately after cooling the melt from 85 °C down to 50 °C. Within the first 2 min, the crystallization of PCL proceeds already over 6%. The crystallization propagates very quickly and finishes within 20 min. The crystallization of PCL on CaF_2 at 50 °C is too slowly to be in-situ followed by FTIR. Therefore, the crystallization of a ~1 μm thick PCL film on CaF_2 substrate was performed at 40 °C. As presented in Fig. 2(b), even though with a 10 °C decrease of the crystallization temperature, the crystallization of PCL on CaF_2 substrate starts about 2 min after cooling the melt from 85 °C down to 40 °C, implying the need of a *ca.* 2 min induction time for initiating the crystallization. These results manifest that the crystallization of PCL films with identical thicknesses is much faster on PE than on CaF_2 substrate. This should be associated to the existence of a freezing PCL layer on PE substrate, which has been confirmed to start the crystallization of PCL at temperatures far above 50 °C (*cf.* Fig. S7 of Ref. [34]).

It should be noted that the crystallization kinetics is most widely analyzed by Avrami model, in which the following equations have frequently been used:

$$(A_t - A_0)/(A_\infty - A_0) = 1 - \exp(-k \times t^n) \tag{1}$$

$$\ln[-\ln((A_\infty - A_t)/(A_\infty - A_0))] = \ln(k) + n\ln(t) \tag{2}$$

$$t_{1/2} = (\ln2/k)^{1/n} + t_0 \tag{3}$$

where n is the Avrami exponent, k is the crystallization rate constant, $t_{1/2}$ is the half-crystallization time and t_0 is the induction time. According the results shown in Fig. 2, the related Avrami plots have been obtained and presented in Fig. 3. From Fig. 3(a), one can see that the best least-squares fitting of Avrami equation to the experimental data of PCL film isothermally crystallized between PE substrates at 50 °C gives an Avrami exponent (n) of ~1.62. It is widely accepted that the n is related to the nucleation type and the crystal growth geometry. For heterogeneous nucleation, a value of n~2 is typical for a two-dimensional crystal growth characteristic for thin film crystallization. For the PCL grown on CaF_2 (Fig. 3b), a value of n~3 reflects most likely a two-dimensional crystal growth under homogeneous nucleation or a three-dimensional crystal growth through heterogeneous nucleation. Moreover, the crystallization rate constant (k) of *ca.* 0.02 for PCL/PE and 1×10^{-3} for PCL/CaF_2 systems indicates also a much faster crystallization PCL on PE than on CaF_2 substrate. This is further supported by the shorter half crystallization time ($t_{1/2}$) of about 8.9 min for PCL/PE at 50 °C than 12.7 min for PCL/CaF_2 at 40 °C.

To display the film thickness dependence of PCL crystallization kinetics in PCL/PE and PCL/CaF_2 systems, the time-dependent relative crystallinity changes and related Avrami
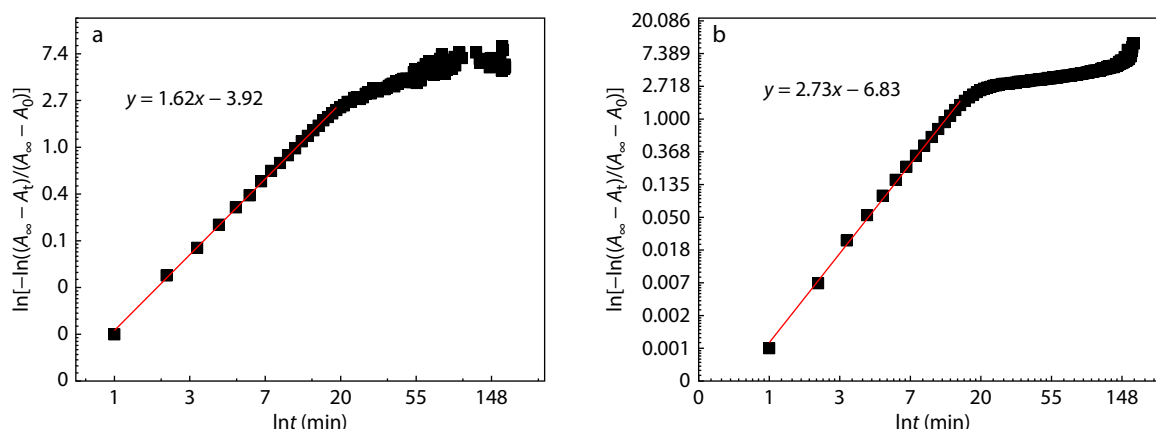
Zhang, H. et al. / Chinese J. Polym. Sci. 2023, 41, 778–786

781

Fig. 3 Avrami plots of a PCL film with 1 μm in thickness sandwiched between two oriented PE substrates during isothermal crystallization at 50 °C (a) and on CaF_2 substrate during isothermal crystallization at 40 °C (b). The solid lines in red color are the best fit of the Avrami equation to the experimental data.

plots of PCL films with different thicknesses sandwiched between two oriented PE substrates or on CaF_2 substrate during isothermal crystallization at 50 and 40 °C, respectively, are presented in electric supplemental information (ESI). Fig. 4 shows the thickness-dependent n, K and $t_{1/2}$ variations with related parameters summarized in Table 1. From Fig. 4(a) and Table 1, we can see that the n value for PCL/PE system increases slightly with increasing PCL film thickness. A maximum value of around 1.6 is reached when the film thickness is over 1 μm, which is obviously smaller than the PCL grown on CaF_2 surface (~3), indicating the different nucleation type and crystal growth manner. The film-thickness-dependent crystallization rate constant of PCL sandwiched between oriented PE thin films and on CaF_2 substrate are presented in Fig. 4(b). Clearly, it decreases with increasing film thickness for PCL/PE system, while increases with increasing film thickness for PCL/CaF_2 system. The results of half crystallization time agree well with that of crystallization rate constant. As presented in

Fig. 4(c), it increases with increasing film thickness for PCL/PE system, while decreases with increasing film thickness for PCL/CaF_2 system.

The above experimental results clearly indicate an opposite film thickness dependence of PCL crystallization kinetics at PE and CaF_2 substrates. This may be understood in the following way. Generally, for thin and ultrathin polymer films, the confinement effect will hinder the crystallization of them.[37–44] For example, it has been reported that the crystallization of poly(di-*n*-hexyl silane) in spin-cast ultrathin films thinner than 15 nm is substantially hindered while gets faster and faster with the increase of film thickness from 15 nm to 50 nm.[37,38] For poly(ethylene oxides) film with thickness smaller than 250 nm crystallized on different silicon substrates, except for a steadily decreased crystallinity, a progressively slowdown crystallization kinetics with decreasing thickness is also observed.[39,40] Similar constrained crystallization phenomenon has been observed for PCL as well.[42,43] It
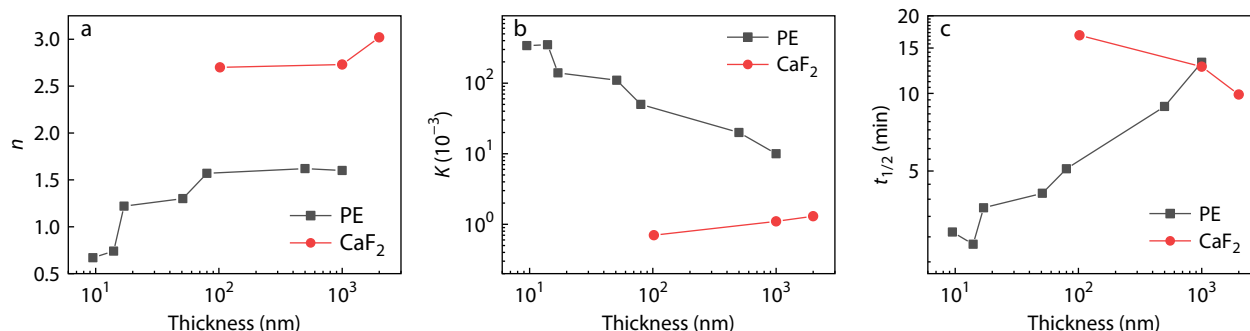

Fig. 4 Thickness dependence of (a) n, (b) K, and (c) $t_{1/2}$ parameters of PCL crystallized on PE at 50 °C and on CaF_2 at 40 °C.

Table 1 Kinetic parameters of PCL with various thicknesses crystallized in PCL/PE and PCL/CaF_2 samples.

Substrates	PE [a]							CaF_2		
Thickness (nm)	9.5	14	17	51	80	500	1000	102	1000	2000
$t_{1/2}$ (min)	2.9	2.6	3.6	4.1	5.1	8.9	13.2	16.8	12.7	9.9
n	0.67	0.74	1.22	1.30	1.57	1.62	1.60	2.7	2.73	3.02
K ($\times10^{-3}$)	340	350	140	110	50	20	10	0.7	1.1	1.3

[a] The thickness of PCL sandwiched between two PE layers is taken as half of the film thickness.

has been reported that both the morphology and growth rate of PCL vary with film thickness. A nonlinear and slower growth of distorted PCL crystals has been recognized. The decreased crystal growth rate with film thickness is often explained by reduced diffusion of polymer chains or chain segments from melt to crystal growth front or decrease of the number of nuclei with decreasing film thickness.[58] Taking all these into account, for the PCL on CaF_2 substrate, there should be a constrained layer directly connected with the CaF_2. The confinement effect results in a very slow crystallization rate of this layer. With increasing film thickness, crystallization of the melt out of this layer gets quicker. This makes an increase of the overall PCL crystallization rate. It should be noted that a relationship between growth rate (G) and film thickness (d) of $G_d = G_\infty \times (1 - a/d)$ has been established for isotactic polystyrene.[44] This validates actually also for the PCL grown on CaF_2. As presented in Fig. 5, when using $1/t_{1/2}$ to characterize the overall crystallization rate, the crystallization rate of PCL on CaF_2 is indeed in proportion to the film thickness d.

The situation of PCL crystallized on PE substrate is different. Except for a decreased crystallization rate with increasing film thickness, non-linear relationship exists between crystallization rate and film thickness (Fig. 5). This reflects a different crystallization mechanism. When crystallizing the PCL on highly oriented PE substrate, either from melt or solution, parallel aligned edge-on PCL lamellar structure is always obtained through epitaxial crystallization.[45,46] The oriented arrangement of PCL chains from melt occurs even at temperatures higher than its nominal melting point. The pre-orientation of molecular chains can promote the nucleation during cooling and accelerates the crystallization tremendously, which ensures a quick crystallization of PCL during cooling at higher temperature.[26] Such interfacial layer with pre-oriented molecular chains or chain segments may in a sense be the same as a freezing layer as denoted by Thurn-Albrecht et al.[34] The crystallization of PCL in the freezing layer is confirmed to start very quickly and at higher temperature, since it can speed up nucleation significantly, or in other words can act as a kind of "ideal nucleus" to initiate crystallization. It should be noted that the PCL freezing layer results actually

from the intrinsic interaction of it with the substrate. There should exist a critical thickness of it. In this case, the crystallization of the melt only within the freezing layer will be remarkably accelerated. Further crystallization of the PCL melts out of the freezing layer is then initiated by the early formed parallel aligned lamellar crystals in freezing layer through homoepitaxial secondary nucleation, i.e., a process of molecular chain or chain segment diffusion from melt to the crystal growth front and packing of them into the crystal lattice, which makes the similar lamellar orientation. Since the secondary nucleation requires an activation process, the crystallization of the PCL out of the freezing layer slows then tremendously down, which reduces the overall crystallization rate of PCL. Assuming a fixed thickness of the freezing layer, the contribution of the fast-crystallizing freezing layer to the overall crystallization rate is then constant regardless of film thickness. The contribution of homoepitaxial secondary crystallization rate to the overall one enhances, however, with increasing film thickness, and therefore leads to an inverse relationship between crystallization rate and film thickness d.

Moreover, from the crystallization rate constants and $t_{1/2}$ shown in Table 1, it is noted that the crystallization behavior of PCL films thinner than 28 nm is essentially the same, while the crystallization of PCL films with thickness larger than 34 nm deviates substantially from those thinner than 28 nm. This may suggest that the thickness of freezing layer intrinsically affected by the PE substrate is in the range of 14–17 nm, which agrees well with the values of PCL on graphite and MoS_2 substrates given by Thurn-Albrecht et al.[33–35] We speculate that this critical freezing layer thickness may correspond to some intrinsic spatial dimensions of the PCL chains, such as the radius of gyration (R_g). To verify whether the critical thickness correlates to the R_g or not, the R_g of the used PCL sample is calculated according to Eq. (4):[59]

$$R_g = \frac{b\sqrt{C_\infty \times (M_w/M_0)}}{\sqrt{6}} \tag{4}$$

where b is the monomer length having a value of 0.7 nm for PCL,[60] C_∞ is the Flory's characteristic ratio with a value of 4.9,[61] M_w and M_0 are the weight-averaged molecular weight and molar mass of a monomer unit, respectively. The used PCL sample has an M_w of 69 kDa with the mass of one monomer unit of 114 g/mol. Thus, an R_g of about 15.6 nm is obtained, which falls well within the range of 14–17 nm. This may imply the existence of a correlation between the R_g of used PCL material and the freezing PCL layer thickness caused by the PE substrate.

Actually, the R_g as a characteristic parameter for discussing the crystallization of thin and ultrathin polymer films near a solid surface has already been used in the literatures.[37,40] For example, Qiao and coworkers reported that the ultrathin PCL film with thickness close to R_g could not crystallize, while a remarkable change in crystalline morphology was found for films with a thickness of around $2R_g$.[62] This deviates obviously from the results of PCL grown on PE substrate presented here since the ultrathin PCL films even thinner than R_g, for example, with a thickness of only about 19/2=9.5 nm, can crystallize on the ordered PE substrate. The divergent crystallization capacity of PCL ultrathin films on the solid surfaces with and without epitaxial abilities may be virtually caused by the same adhesion phenomenon of polymer chains or chain
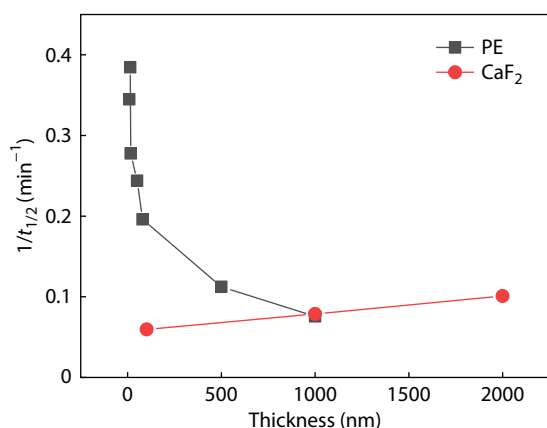

Fig. 5   Plots of $1/t_{1/2}$ against film thickness of PCL sandwiched between PE films crystallized at 50 °C and on CaF_2 substrate crystallized at 40 °C.
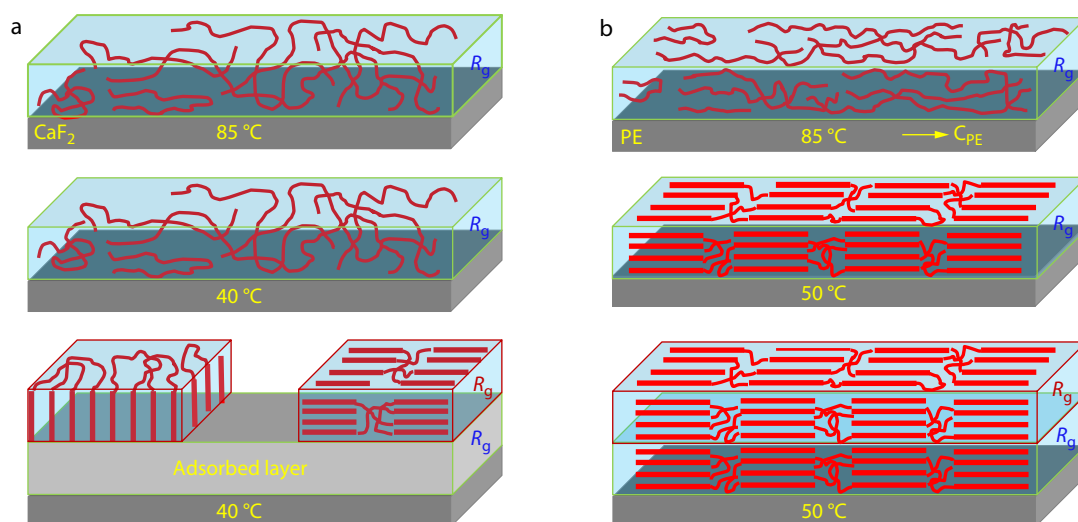
Fig. 6   Schematic view of possible PCL chain arrangement at a solid surface without epitaxial capacity as CaF$_2$ (a) and with epitaxial ability like oriented PE (b). The yellow arrow in part (b) indicates the molecular chain direction of the used PE substrate. The PCL chains in melt at CaF$_2$ surface are random coils (top panel of part a). By cooling the film to crystallization temperature, the PCL chains in the interfacial layer of R_g in thickness keep their original random coil conformation due to strong adsorption of them by the substrate, and therein the crystallization in this layer is tremendously depressed or even totally inhibited (middle panel of part a). With further increase of film thickness, the PCL chains outside the strongly adsorbed layer can crystallize with low rate (bottom panel of part a) with different morphologies (*e.g.*, flat-on and edge-on shown in left and right parts, respectively). The PCL chains at PE substrate are pre-oriented as reported in Ref. [34] (top panel of part b), which leads to the formation of a freezing PCL layer with ordered structure even above the melting point of PCL and therefore initiates the immediate crystallization of PCL at 50 °C (middle panel of part b). The PCL chains outside the strongly adsorbed layer crystallize continuously and slowly through homoepitaxial secondary nucleation (bottom panel of part b).

segments onto the substrate surface in different manners. It has been reported that there exists an irreversibly adsorbed layer at substrate surface with thickness comparable to R_g of the polymer chains.[63] Both mobility and conformation of the polymer chains in the adsorbed interface layer can be altered. It is the changes in chain mobility and conformation that result in the divergent crystallization behavior of a polymer at different solid substrates. Generally, the mobility of molecular chain segments within the interfacial adsorbed layer is reduced greatly due to the mutual interaction, as manifested by the increased glass transition temperature of polymers.[40,41] At a solid surface without epitaxy capacity, as depicted in top panel of Fig. 6(a), the adsorbed polymer chains in the interfacial region exhibit a random coil arrangement like in its bulk. In this case, the reduction in mobility of molecular chain segments within the adsorbed interfacial layer of R_g in thickness depresses or even inhibits the crystallization of this ultrathin layer when cooled down to crystallization temperature, see middle panel of Fig. 6(a). The effect of substrate toward the polymer chains, *i.e.*, the substrate-polymer interaction strength, decreases gradually with the polymer chains deviating from the interface as film thickness increases. Consequently, the materials outside the strongly adsorbed interfacial layer can crystallize but with very low nucleation and crystal growth rate. In this case, Hu *et al.*[64] confirmed through dynamic Monte Carlo simulation that the morphology depends generally on the substrate-polymer interaction strength and crystallization condition, such as flat-on lamellar crystals shown in bottom left of Fig. 6(a) or/and edge-on lamellar crystals shown in bottom right of Fig. 6(a), both of them have been reported in literatures.[42,43] With further increase of the film thickness, the effect of substrate fades out.

The layers far away from the interface then crystallize in the similar way as bulk material. This results in an increased overall crystallization rate. There exists a critical thickness that the contribution of substrate-adsorbed layer to the overall crystallization kinetics can be neglected. As a result, films thicker than this critical thickness do not illustrate the substrate effect.

On the other hand, as schematically described in Fig. 6(b), the PCL chains or chain segments in the adsorbed interfacial layer caused by PE, considered here as the freezing layer as proposed by Thurn-Albrecht that can stabilize the crystal structure well above the bulk melting temperature of PCL or endow an oriented chain organization at temperatures higher than the melting point of PCL, which can serve as self-nuclei and induce crystallization of PCL more easily than the bulk crystallization.[65] These early formed PCL crystals can also trigger the crystallization of PCL out of the freezing layer through homoepitaxial secondary nucleation with a slower rate due to the requirement of an activation process. Since the overall crystallization kinetics is an average of the PCL within and out of the freezing layer and the contribution of homoepitaxial secondary crystallization to the overall crystallization rate gets bigger and bigger with increasing film thickness, the overall crystallization rate decreases thus with increasing film thickness. This well explains the reduced crystallization kinetics of PCL on PE with increasing thickness.

CONCLUSIONS

In summary, the film-thickness-dependent crystallization kinetics of PCL on CaF$_2$ and oriented PE substrates was studied by FTIR spectroscopy using the carbonyl absorption band at

1724 cm^{-1}. The results show that the crystallization of PCL with similar thickness is much faster on oriented PE substrate than at CaF$_2$ surface. The quick PE-induced crystallization of PCL is related to the existence of a freezing layer, which immediately produces the simultaneous growth of parallel aligned PCL lamellae with molecular chain along PE molecular chain direction.

The influence of film thickness on the crystallization kinetics of PCL on PE substrate is also different from that on CaF$_2$ substrate. The overall crystallization rate of PCL on CaF$_2$ substrate accelerates with increasing film thickness, while that on PE substrate gets slower and slower with film thickness. For the PCL on CaF$_2$, the mobility of PCL chain segments in the adsorbed layer decreases remarkably, which reduces or even inhibits the crystallization of it. The gradual elimination of the substrate effect for the PCL chains away from the CaF$_2$ substrate with increasing film thickness results in an increment of the overall crystallization kinetics. In the contrary, for the PCL-PE system, the existence of a PCL freezing layer at the PE surface with pre-oriented chain structure promotes the crystallization of it greatly. The further growth of PCL crystals out of the freezing layer with random coil conformation triggered by early formed PCL lamellar crystals through homoepitaxial secondary nucleation requires an activation process and is slower than that in the freezing layer. Consequently, a decrement of crystallization kinetics with increasing film thickness is observed.

Moreover, the thickness of the PCL layer with fastest crystallization rate on PE is estimated to be in the range of 14–17 nm, which is similar to the reported freezing layer thickness of PCL on graphite and MoS$_2$ substrates. Interestingly, the R_g of the used PCL material falls also in this range. This may suggest the existence of a correlation between the R_g of the polymers and the freezing layer thickness, which warrants a further study.

NOTES

The authors declare no competing financial interest.

![E] Electronic Supplementary Information

Electronic supplementary information (ESI) is available free of charge in the online version of this article at http://doi.org/10.1007/s10118-023-2929-z.

ACKNOWLEDGMENTS

REFERENCES

1   Corradini, P.; Guerra, G. Polymorphism in polymers. In *Macromolecules: Synthesis, Order and Advanced Properties*, Springer Berlin Heidelberg: Berlin, Heidelberg, **1992**; pp. 183-217.

2   Lovinger, A. J. Ferroelectric polymers. *Science* **1983**, *220*, 1115–1121.

3   Liu, Y.; Li, C.; Ren, Z.; Yan, S.; Bryce, M. R. All-organic thermally activated delayed fluorescence materials for organic light-emitting diodes. *Nat. Rev. Mater.* **2018**, *3*, 1–20.

4   Smith, P.; Lemstra, P. J. Ultra-high-strength polyethylene filaments by solution spinning/drawing. *J. Mater. Sci.* **1980**, *15*, 505–514.

5   Li, C.; Xu, Y.; Liu, Y.; Ren, Z.; Ma, Y.; Yan, S. Highly efficient white-emitting thermally activated delayed fluorescence polymers: synthesis, non-doped white OLEDs and electroluminescent mechanism. *Nano Energy* **2019**, *65*, 104057.

6   Li, C.; Ren, Z.; Sun, X.; Li, H.; Yan, S. Deep-blue thermally activated delayed fluorescence polymers for non-doped solution processed organic light emitting diodes. *Macromolecules* **2019**, *52*, 2296–2303.

7   Zheng, Y.; Tee, H.T.; Wei, Y.; Wu, X.; Mezger, M.; Yan, S.; Landfester, K.; Wagener, K.; Wurm, F.R.; Lieberwirth, I. On the structure and thermal properties of precision polyphosphoesters. *Macromolecules* **2016**, *49*, 1321–1330.

8   Wen, G.; Ren, Z.; Sun, D.; Zhang, T.; Liu, L.; Yan, S. Synthesis of alternating copolysiloxane with terthiophene and perylenediimide derivative pendants for involatile WORM memory device. *Adv. Funct. Mater.* **2014**, *24*, 3446–3455.

9   Dong, H.; Li, H.; Wang, E.; Yan, S.; Zhang, J.; Yang, C.; Takahashi, I.; Nakashima, H.; Torimitsu, K.; Hu, W. Molecular orientation and field-effect transistors of a rigid rod conjugated polymer thin films. *J. Phys. Chem. B* **2009**, *113*, 4176–4180.

10 Deng, L. F.; Zhang, X. X.; Zhou, D.; Tang, J. H.; Lei, J.; Li, J. F.; Li, Z. M. Better choice: linear long chains rather than branched ones to improve mechanical performance of polyethylene through generating shish-kebabs. *Chinese J. Polym. Sci.* **2020**, *38*, 715–729.

11 Briseno, A. L.; Aizenberg, J.; Han, Y. J.; Penkala, R. A.; Moon, H.; Lovinger, A. J.; Kloc, C.; Bao, Z. Patterned growth of large oriented organic semiconductor single crystals on self-assembled monolayer templates. *J. Am. Chem. Soc.* **2005**, *127*, 12164–12165.

12 Xin, R.; Zhang, J.; Sun, X.; Li, H.; Ren, Z.; Yan, S. Polymorphic behavior and phase transition of poly(1-butene) and its copolymers. *Polymers* **2018**, *10*, 556.

13 Brinkmann, M. Structure and morphology control in thin films of regioregular poly(3-hexylthiophene). *J. Polym. Sci., Part B: Polym. Phys.* **2011**, *49*, 1218–1233.

14 Hu, J.; Xin, R.; Hou, C.; Yan, S. Preparation and self-repairing of highly oriented structures of ultrathin polymer films. *Macromol. Chem. Phys.* **2019**, 1800478.

15 Li, S.; Sun, X.; Li, H.; Yan, S. The crystallization behavior of biodegradable polymer in thin film. *Eur. Polym. J.* **2018**, *102*, 238–253.

16 Wittmann, J. C.; Smith, P. Highly oriented thin films of poly(tetrafluoroethylene) as a substrate for oriented growth of materials. *Nature* **1991**, *352*, 414–417.

17 Brinkmann, M.; Wittmann, J. C. Orientation of regioregular poly(3-hexylthiophene) by directional solidification: a simple method to reveal the semicrystalline structure of a conjugated polymer. *Adv. Mater.* **2006**, *18*, 860–863.

18 Brinkmann, M.; Rannou, P. Effect of molecular weight on the structure and morphology of oriented thin films of regioregular poly(3-hexylthiophene) grown by directional epitaxial solidification. *Adv. Funct. Mater.* **2007**, *17*, 101–108.

19 Brinkmann, M. Directional epitaxial crystallization and tentative crystal structure of poly(9,9'-di-*n*-octyl-2,7-fluorene). *Macromolecules* **2007**, *40*, 7532–7541.

20 Hamidi-Sakr, A.; Schiefer, D.; Covindarassou, S.; Biniek, L.; Sommer, M.; Brinkmann, M. Highly oriented and crystalline films of a phenyl-substituted polythiophene prepared by epitaxy:

Structural model and influence of molecular weight. *Macromolecules* **2016**, *49*, 3452–3462.

21 Zhou, H.; Yan, S. Can the structures of semicrystalline polymers be controlled using interfacial crystallographic interactions. *Macromol. Chem. Phys.* **2013**, *214*, 639–653.

22 Li, Y.; Guo, Z.; Xue, M.; Yan, S. Epitaxial recrystallization of *i*PBU in form II on an oriented *i*PS film initially induced by oriented form I *i*PBu. *Macromolecules* **2019**, *52*, 4232–4239.

23 Liu, J.; Wang, J.; Li, H.; Shen, D.; Zhang, J.; Ozaki, Y.; Yan, S. Epitaxial crystallization of isotactic poly(methyl methacrylate) on highly oriented polyethylene. *J. Phys. Chem. B* **2006**, *110*, 738–742.

24 Dong, H.; Li, H.; Wang, E.; Wei, Z.; Xu, W.; Hu, W.; Yan, S. Ordering rigid rod conjugated polymer molecules for high performance photoswitchers. *Langmuir* **2008**, *24*, 13241–13244.

25 Li, H.; Yan, S. Surface-induced polymer crystallization and the resultant structures and morphologies. *Macromolecules* **2011**, *44*, 417–428.

26 Hu, J.; Xin, R.; Hou, C.; Yan, S.; Liu, J. Direct comparison of crystal nucleation activity of pcl on patterned substrates. *Chinese J. Polym. Sci.* **2019**, *37*, 693–699.

27 Wittmann, J. C.; Lotz, B. Polymer decoration: The orientation of polymer folds as revealed by the crystallization of polymer vapors. *J. Polym. Sci., Part B: Polym. Phys.* **1985**, *23*, 205–226.

28 Wittmann, J. C.; Lotz, B. Epitaxial crystallization of polymers on organic and polymeric substrates. *Prog. Polym. Sci.* **1990**, *15*, 909–948.

29 Brinkmann, M.; Hartmann, L.; Kayunkid, N.; Djurado, D. Understanding the structure and crystallization of regioregular poly(3-hexylthiophene) from the perspective of epitaxy. *Adv. Polym. Sci.* **2014**, *265*, 83–106.

30 Yan, S.; Yang, D.; Petermann, J. Controlling factors for the occurrence of heteroepitaxy of polyethylene on highly oriented isotactic polypropylene. *Polymer* **1998**, *39*, 4569–4578.

31 Löhmann, A.-K.; Henze, T.; Thurn-Albrecht, T. Direct observation of prefreezing at the interface melt-solid in polymer crystallization. *Proc. Natl. Acad. Sci. U. S. A.* **2014**, *111*, 17368–17372.

32 Tariq, M.; Dolynchuk, O.; Thurn-Albrecht, T. Effect of substrate interaction on thermodynamics of prefreezing. *Macromolecules* **2019**, *52*, 9140–9148.

33 Tariq, M.; Dolynchuk, O.; Thurn-Albrecht, T. Independent variation of transition temperature and prefrozen layer thickness at the prefreezing transition. *J. Phys. Chem. C* **2020**, *124*, 26184–26192.

34 Flieger, A.-K.; Schulz, M.; Thurn-Albrecht, T. Interface-induced crystallization of polycaprolactone on graphite *via* first-order prewetting of the crystalline phase. *Macromolecules* **2018**, *51*, 189–194.

35 Dolynchuk, O.; Tariq, M.; Thurn-Albrecht, T. Phenomenological theory of first-order prefreezing. *J. Phys. Chem. Lett.* **2019**, *10*, 1942–1946.

36 Tariq, M.; Thurn-Albrecht, T.; Dolynchuk, O. Heterogeneous crystal nucleation from the melt in polyethylene oxide droplets on graphite: kinetics and microscopic structure. *Crystals* **2021**, *11*, 924.

37 Frank, C.; Rao, V.; Despotopoulou, M.; Pease, R.; Hinsberg, W.; Miller, R.; Rabolt, J. Structure in thin and ultrathin spin-cast polymer films. *Science* **1996**, *273*, 912–915.

38 Despotopoulou, M.; Frank, C.; Miller, R.; Rabolt, J. Kinetics of chain organization in ultrathin poly(di-*n*-hexylsilane) films. *Macromolecules* **1996**, *29*, 5797–5804.

39 Schönherr, H.; Frank, C. Ultrathin films of poly(ethylene oxides) on oxidized silicon. 1. Spectroscopic characterization of film structure and crystallization kinetics. *Macromolecules* **2003**, *36*,

40 Schönherr, H.; Frank, C. Ultrathin films of poly(ethylene oxides) on oxidized silicon. 2. *In situ* study of crystallization and melting by hot stage AFM. *Macromolecules* **2003**, *36*, 1199–1208.

41 Prud'homme, R. E. Crystallization and morphology of ultrathin films of homopolymers and polymer blends. *Prog. Polym. Sci.* **2016**, *54-55*, 214–231.

42 Mareau, V. H.; Prud'homme, R. E. *In-situ* hot stage atomic force microscopy study of poly(ε-caprolactone) crystal growth in ultrathin films. *Macromolecules* **2005**, *38*, 398–408.

43 Mamun, A.; Mareau, V. H.; Chen, J.; Prud'homme, R. E. Morphologies of miscible PCL/PVC blends confined in ultrathin films. *Polymer* **2014**, *55*, 2179–2187.

44 Taguchi, K.; Miyaji, H.; Izumi, K.; Hoshino, A.; Miyamoto, Y.; Kokawa, R. Growth shape of isotactic polystyrene crystals in thin films. *Polymer* **2001**, *42*, 7443–7447.

45 Yan, C.; Li, H.; Zhang, J.; Ozaki, Y.; Shen, D.; Yan, D.; Shi, A. C.; Yan, S. Surface-induced anisotropic chain ordering of polycarprolactone on oriented polyethylene substrate: epitaxy and soft epitaxy. *Macromolecules* **2006**, *39*, 8041–8048.

46 Chang, H.; Zhang, J.; Li, L.; Wang, Z.; Yang, C.; Takahashi, I.; Ozaki, Y.; Yan, S. A study on the epitaxial ordering process of the polycaprolactone on the highly oriented polyethylene substrate. *Macromolecules* **2010**, *43*, 362–366.

47 Zhang, Y.; Lu, Y.; Duan, Y.; Zhang, J.; Yan, S.; Shen, D. Reflection-absorption infrared spectroscopy investigation of the crystallization kinetics of poly(ethylene terephthalate) ultrathin films. *J. Polym. Sci., Phys. Ed.* **2004**, *42*, 4440–4447.

48 Zhang, Y.; Zhang, J.; Lu, Y.; Duan, Y.; Yan, S.; Shen, D. Glass transition temperature determination of poly(ethylene terephthalate) thin films using reflection-absorption FTIR. *Macromolecules* **2004**, *37*, 2532–2537.

49 Duan, Y.; Zhang, J.; Shen, D.; Yan, S. *In situ* FTIR studies on the cold-crystallization process and multiple melting behavior of isotactic polystyrene. *Macromolecules* **2003**, *36*, 4874–4879.

50 Zhang, J.; Duan, Y.; Shen, D.; Yan, S.; Noda, I.; Ozaki, Y. 2D FTIR spectroscopic studies on the structure change in the induction period of the cold-crystallization of isotactic polystyrene. *Macromolecules* **2004**, *37*, 3292–3298.

51 Petermann, J.; Gohil, R. M. A new method for the preparation of high modulus thermoplastic films. *J. Mater. Sci.* **1979**, *14*, 2260–2264.

52 Yan, S. Origin of oriented recrystallization of carbon coated pre-oriented ultra-thin polymer films. *Macromolecules* **2003**, *36*, 339–345.

53 Li, H.; Liu, D.; Bu, X.; Zhou, Z.; Ren, Z.; Sun, X.; Reiter, R.; Yan, S.; Reiter, G. Formation of asymmetric leaf-shaped crystals in ultrathin films of oriented polyethylene molecules resulting from high-temperature relaxation and recrystallization. *Macromolecules* **2020**, *53*, 346–354.

54 Zhou, H.; Jiang, S.; Yan, S. Epitaxial crystallization of poly(3-hexylthiophene) on a highly oriented polyethylene thin film from solution. *J. Phys. Chem. B* **2011**, *115*, 13449–13454.

55 An, Y.; Jiang, S.; Yan, S.; Sun J.R.; Chen, X. Crystallization behavior of polylactide on highly oriented polyethylene thin films. *Chinese J. Polym. Sci.* **2011**, *29*, 513–519.

56 Liu, J.; Li, H.; Yan, S.; Xiao, Q.; Petermann, J. Epitaxial- and trans-crystallization of PCL on the highly oriented PE substrates. *Colloid Polym. Sci.* **2003**, *281*, 601–607.

57 Phillipson, K.; Hay, J. N.; Jenkins, M. J. Thermal analysis FTIR spectroscopy of poly(ε-caprolactone). *Thermochimica Acta* **2014**, *595*, 74–82.

58 Massa, M. V.; Dalnoki-Veress, K. Homogeneous crystallization of poly(ethylene oxide) confined to droplets: the dependence of the crystal nucleation rate on length scale and temperature. *Phys.*

Rev. Lett. **2004**, *92*, 255509.

59 Rubinstein, M.; Colby, R. H. in *Polymer Physics*. Oxford University Press: New York, **2004**.

60 Xu, F.; Zhang, P.; Zhang, J.; Yu, C.; Yan, D.; Mai, Y. Crystallization-driven two-dimensional self-assembly of amphiphilic PCL-*b*-PEO coated gold nanoparticles in aqueous solution. *ACS Macro Lett.* **2018**, *7*, 1062–1067.

61 Yuan, L.; Hamidi, N.; Smith, S.; Clemons, F.; Hamidi, A.; Tang, C. Molecular characterization of biodegradable natural resin acid-substituted polycaprolactone. *Eur. Polym. J.* **2015**, *62*, 43–50.

62 Qiao, C.; Zhao, J.; Jiang, S.; Ji, X.; An, L.; Jiang, B. Crystalline morphology evolution in pcl thin films. *J. Polym. Sci., Part B: Polym. Phys.* **2005**, *43*, 1303–1309.

63 Jouault, N.; Moll, J. F.; Meng, D.; Windsor, K.; Ramcharan, S.; Kearney, C.; Kumar, S. K. Bound polymer layer in nanocomposites. *ACS Macro Lett.* **2013**, *2*, 371–374.

64 Ma, Y.; Hu, W.; Reiter, G. Lamellar crystal orientations biased by crystallization kinetics in polymer thin films. *Macromolecules* **2006**, *39*, 5159–5164.

65 Li, H.; Sun, X.; Wang, J.; Yan, S.; Schultz, J.M. On the development of special positive isotactic polypropylene spherulites. *J. Polym. Sci., Phys. Ed.* **2006**, *44*, 1114–1121.